IEEE *Access*

RESEARCH ARTICLE

Fine Beam Tracking Using Spatio–Temporal Interpolation in Wireless Power Transfer Systems

KI-WON PARK[1], (Student Member, IEEE), GIL-MO KANG[2],
HYEON MIN KIM[2], (Member, IEEE), AND OH-SOON SHIN[1,2], (Member, IEEE)
[1]School of Electronic Engineering, Soongsil University, Seoul 06978, South Korea
[2]Department of Information Communication Convergence Technology, Soongsil University, Seoul 06978, South Korea

Corresponding author: Oh-Soon Shin (osshin@ssu.ac.kr)

ABSTRACT The use of transmit beamforming in a radio-frequency wireless power transfer (WPT) system can improve the energy transmission efficiency by concentrating the transmit power in the angle of departure (AoD). Optimal beamforming requires information regarding the AoD or the channel between the transmitter and receiver. A previously proposed WPT system continually estimates the optimal AoD using custom-designed pilot signals, which are known as beam-steered pilot signals and are transmitted periodically at every frame. Herein, we propose a spatio–temporal interpolation technique to improve the accuracy of beam tracking for such a WPT system. Specifically, thin-plate spline interpolation is adopted in the space domain to overcome the limited angular resolution of the beam-steered pilot signals in a three-dimensional channel. In the time domain, polynomial interpolation is performed to track the changing AoD during consecutive frames. Numerical results show that the proposed technique can improve the WPT efficiency as well as the mean square error performance of the beamforming weight vector.

INDEX TERMS Beamforming, pilot signals, spatio–temporal interpolation, wireless power transfer (WPT).

I. INTRODUCTION

Recently, massive Internet of Things (IoT), which is one of the target scenarios of the fifth generation mobile communication, has garnered increasing attention. Massive IoT scenarios aim to support effective communication between massive number of connected devices [1], [2], [3], [4]. For massive IoT to be effectively deployed, it is important to develop a technology that supplies the power required by IoT devices, as well as an efficient multiple access technology that supports massive devices [5], [6], [7]. To solve the power supply problem in IoT devices, one can adopt wireless power transfer (WPT) technology, which is classified into magnetic induction, magnetic resonance, and radio-frequency (RF) radiation methods. In the magnetic induction method, miniaturization is difficult to accomplish owing to the short-range power transmission that is within 1 cm, as well as heat issues.

The associate editor coordinating the review of this manuscript and approving it for publication was Claudio Curcio[ID].

In the magnetic resonance method, the charging distance is severely limited, and coupling and stability problems occur when many devices are used in a large space [8], [9], [10], [11]. Therefore, in this study, we investigated an RF radiation method that enables relatively long-distance WPT to mobile receivers [12], [13]. The RF radiation method can also be advanced to simultaneous wireless information and power transfer (SWIPT) systems [14], which incorporate WPT into wireless communications.

In the RF radiative WPT system, transmit beamforming is an effective method for improving energy transmission efficiency by concentrating the transmit power in the direction of the receiving device. In particular, a phased-array antenna can steer a beam toward a desired angle of departure (AoD) by adjusting the phases of the individual antenna elements. Therefore, the phased-array antenna can be effectively adopted for WPT, wireless communications, SWIPT, and radar [15], [16], [17], [18]. Optimal beamforming that conveys maximum energy to the receiver adjusts the phases

of the individual antenna elements such that the signal with the same phase reaches the receiver from every individual antenna. To achieve optimal beamforming, the transmitter must be aware of the AoD [19], or equivalently, the channel state information between the transmitter and receiver [20]. The transmitter typically transmits pilot signals known by the receiver to obtain information pertaining to the AoD or channel state [21].

Recently, a simple but effective beam scanning method was proposed to realize beamforming in a WPT system [22]. The beam space was partitioned into several subspaces, and the transmitter transmitted a pilot signal steered in the AoD corresponding to each subspace. Each beam subspace was scanned by changing the AoD of the steered pilot signals. By measuring the received signal strengths corresponding to the pilot signals, the receiver can identify the optimal beam subspace, i.e., the AoD corresponding to the maximum energy reception. Subsequently, the receiver provides the optimal AoD information to the transmitter via a dedicated feedback channel. The accuracy of the beam-scanning scheme is determined by the resolution of the pilot signals in the space and time domains, as the pilot signals are intermittently transmitted for a finite number of quantized beam subspaces [22]. A direct solution for improving the accuracy in the space domain is to increase the number of beam subspaces. However, an increase in the number of beam subspaces will increase the feedback overhead because more bits are required to represent the increased number of beam subspaces. Besides, the receiver mobility deteriorates the accuracy of beam scanning in the time domain. The effect of mobility can be mitigated by reducing the interval between the pilot signals. However, this may undermine the time duration for WPT, thereby decreasing the overall power transfer efficiency.

Herein, we propose a spatio–temporal interpolation technique to improve the beamforming accuracy in both the space and time domains in a WPT system based on beam scanning. The proposed technique estimates the optimal AoD via the thin-plate spline (TPS) interpolation of the received signal strengths, which are associated with a finite number of beam subspaces. The interpolation enhances the resolution of the pilot signals, thereby improving the AoD estimation performance of the transmitter in a three-dimensional (3D) space. Furthermore, polynomial interpolation is employed to track the moving path of the receiver during consecutive time frames, which enables more frequent updates of the steering AoD. Hence, the proposed technique is expected to improve the accuracy of beamforming in both space and time domains. Numerical results are presented to demonstrate the
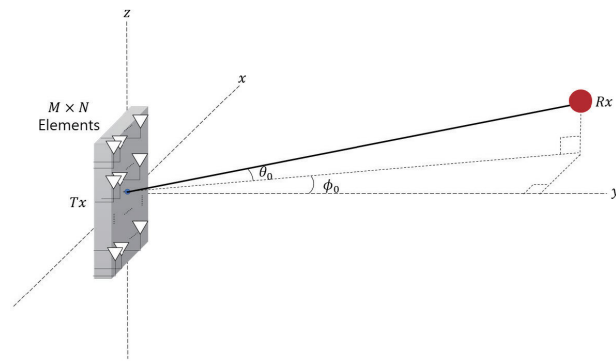

FIGURE 1. WPT system with PAA at transmitter.

effectiveness of the proposed technique in terms of energy transmission efficiency.

The remainder of this paper is organized as follows: Section II describes the signal model for a WPT system and briefly reviews the beam scanning method proposed in [22]. In Section III, the spatio–temporal interpolation technique proposed herein for improving the accuracy of beam scanning in space and time domains is described. The numerical results and conclusions are presented in Sections IV and V, respectively.

II. SYSTEM MODEL

We consider a radiative WPT system to IoT devices with a planar array antenna (PAA) installed at the transmitter, as illustrated in Fig. 1. In a PAA composed of $N_t(= MN)$ antennas, M antennas along the x-axis and N antennas along the z-axis are uniformly placed with a spacing d of one-half the wavelength, i.e., $d = \lambda/2$. This antenna configuration allows the PAA to form a directive beam with a narrow main beam in a 3D space. The receiver is assumed to be equipped with a single antenna. In the following subsections, we present the signal model for WPT and provide a brief review of the beam scanning scheme proposed in [22].

A. SIGNAL MODEL

The beamforming weights can be represented as an $M \times N$ matrix $\mathbf{W}$, which is defined as (1), shown at the bottom of the page, where θ_0 and ϕ_0 are the elevation angle and azimuth angle between the transmitter and receiver, respectively, and $k = 2\pi/\lambda$ denotes the angular wave-number. For simplicity of the subsequent representations, we express the beamforming weights as an equivalent $N_t \times 1$ vector $\mathbf{w}$ by stacking the

$$\mathbf{W}(\theta_0, \phi_0) \triangleq \begin{bmatrix} 1 & e^{-jkd(\cos\theta_0\sin\phi_0)} & \cdots & e^{-jkd((M-1)\cos\theta_0\sin\phi_0)} \\ e^{-jkd(\sin\theta_0\cos\phi_0)} & e^{-jkd(\cos\theta_0\sin\phi_0+\sin\theta_0\cos\phi_0)} & \cdots & e^{-jkd((M-1)\cos\theta_0\sin\phi_0+\sin\theta_0\cos\phi_0)} \\ \vdots & \vdots & \ddots & \vdots \\ e^{-jkd((N-1)\sin\theta_0\cos\phi_0)} & e^{-jkd(\cos\theta_0\sin\phi_0+(N-1)\sin\theta_0\cos\phi_0)} & \cdots & e^{-jkd((M-1)\cos\theta_0\sin\phi_0+(N-1)\sin\theta_0\cos\phi_0)} \end{bmatrix} \quad (1)$$
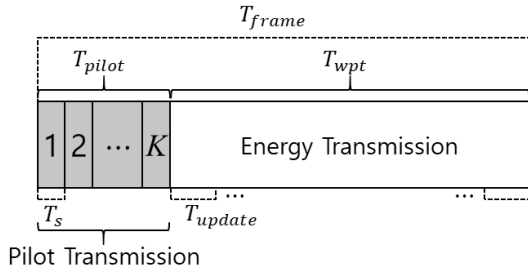
FIGURE 2. Frame structure for WPT.

columns of $\mathbf{W}$:

$$\mathbf{w}(\theta_0, \phi_0) \triangleq [1, \ldots, e^{-jkd((m-1)\cos\theta_0 \sin\phi_0 + (n-1)\sin\theta_0 \sin\phi_0)}, \\ \ldots, e^{-jkd((M-1)\cos\theta_0 \sin\phi_0 + (N-1)\sin\theta_0 \sin\phi_0)}]^T, \tag{2}$$

where $(\cdot)^T$ denotes the transpose operation. Then, the $N_t \times 1$ beamformed signal vector $\mathbf{x}(t)$ at the transmitter can be expressed as $\mathbf{x}(t) = \mathbf{w}s(t)$, where $s(t)$ denotes the transmit energy signal.

Correspondingly, the signal $y(t)$ received at the receiver can be expressed as

$$y(t) = \sqrt{P}\mathbf{h}^H \mathbf{w}s(t) + n(t), \tag{3}$$

where P is the average received power and $\mathbf{h}$ is an equivalent $N_t \times 1$ channel vector constructed by stacking the column of the $M \times N$ channel matrix. $n(t)$ is the additive white Gaussian noise process with a variance of σ^2, and $(\cdot)^H$ the Hermitian transpose. As the energy is typically conveyed on a narrowband tone signal, the channel vector $\mathbf{h}$ can be written as

$$\mathbf{h} = [\gamma_{11} E(\theta_{11}, \phi_{11}) e^{jkr_{11}}, \ldots, \gamma_{mn} E(\theta_{mn}, \phi_{mn}) e^{jkr_{mn}}, \\ \ldots, \gamma_{MN} E(\theta_{MN}, \phi_{MN}) e^{jkr_{MN}}]^T, \tag{4}$$

where θ_{mn} and ϕ_{mn} represent the elevation and azimuth angles, respectively, between the (m, n) antenna element of the PAA and the receive antenna; r_{mn} denotes the distance between the (m, n) antenna element and the receive antenna; γ_{mn} represents the corresponding path loss; $E(\theta, \phi)$ denotes the field pattern of each antenna element, which is assumed to be a dipole antenna with directional linear pattern, i.e., $E(\theta, \phi) = \sqrt{1 - \sin^2\theta \sin^2\phi}, \ \forall \theta, \phi \in [-\pi, \pi]$ [23].

B. BEAM SCANNING METHOD PROPOSED IN [22]
Fig. 2 shows a transmission frame structure for WPT. The frame duration T_{frame} is segmented into a section T_{pilot}, in which a pilot signal is transmitted, and another section T_{wpt}, in which WPT is performed. For beam-steered pilot transmission, the entire beam space is segmented into K subspaces, each of which corresponds to a steered AoD. The beam-steered pilot signals are transmitted toward the K predetermined AoDs, and the signal for each AoD persists for T_s. The beamforming AoD for power transfer is determined

based on feedback received from the receiver in the previous frame.

It is noteworthy that in (4), if the distance r_0 between the transmitter and receiver is sufficient to satisfy the far-field approximation, then one can assume that the azimuth and elevation angles between every antenna element of the PAA and the receive antenna are equal, i.e., $\theta_{mn} = \theta_0, \phi_{mn} = \phi_0$. Therefore, the optimal beamforming AoD is determined solely by θ_0 and ϕ_0. Both the azimuth steering and elevation steering angles for K steered AoDs as well as the corresponding beamforming weight vectors are stored in a codebook. Codebook $\mathcal{C}$, which is a set of beamforming weight vectors corresponding to quantized AoDs of pilot signals, is defined as

$$\mathcal{C} = \{(\theta_i, \phi_j, \mathbf{w}(\theta_i, \phi_j)) : i = 1, 2, \ldots, K_e, j = 1, 2, \ldots, K_a\}. \tag{5}$$

The transmitter sequentially transmits the steered beam toward the beam subspace. If the beam space scanned by the beam-steered pilot signals is uniformly quantized, then the angles θ_i and ϕ_j corresponding to the beam subspace (i, j) can be expressed as

$$\theta_i = \theta_{min} + (i - 1)\Delta\theta, \quad i = 1, 2, \ldots, K_e, \\ \phi_j = \phi_{min} + (j - 1)\Delta\phi, \quad j = 1, 2, \ldots, K_a, \tag{6}$$

where θ_{min} and ϕ_{min} represent the minimum values of the elevation and azimuth angles, respectively; $\Delta\theta$ and $\Delta\phi$ represent the step sizes between adjacent elevation angles and azimuth angles, respectively; K_e and K_a represent the total numbers of elevation and azimuth angles, respectively. The total number of codewords constituting the codebook, i.e., the number of beam subspaces, is $K(= K_e K_a = 2^{b_e + b_a} = 2^b)$, where b_e and b_a denote the numbers of quantization bits for the elevation and azimuth angles, respectively.

The receiver measures the average received signal strength of each beam-steered pilot signal using a rectifier. The received signal strength p_{ij} for the pilot signal corresponding to the AoD (θ_i, ϕ_j) can be expressed as

$$p_{ij} = P|\mathbf{h}^H \mathbf{w}(\theta_i, \phi_j)|^2 E[|s(t)^2|] + \sigma^2, \\ i = 1, 2, \ldots, K_e, j = 1, 2, \ldots, K_a. \tag{7}$$

$\hat{\theta}$ and $\hat{\phi}$, which are associated with the maximum values among the measured K average power values, are identified as being the AoD for the receiver, and the corresponding index are fed back to the transmitter. Note that the index can be represented using $b (= b_e + b_a)$ bits (b_e bits for elevation angle and b_a bits for azimuth angle), and it must be sent every frame. Hence, the feedback requires a dedicated communication link with minimum data rate of b/T_{frame} [bps], which is defined as the feedback overhead.

III. PROPOSED SPATIO–TEMPORAL INTERPOLATION TECHNIQUE
In the conventional beam scanning scheme, the beam weight vector is updated in each frame. Increasing the

beam-scanning resolution increases the pilot overhead as the number of feedback bits increases. In addition, an increase in the pilot interval T_{pilot} within the frame reduces the power transfer interval T_{wpt}, degrading the WPT efficiency, which is defined as the ratio of the received signal power to the transmit signal power. Meanwhile, in the time domain, the capability of the transmitter in reflecting the mobility of the receiver across frames is limited because the beam weight vector, i.e., the AoD, is updated only once every frame. If the frame duration is decreased to achieve more frequent updates, then the ratio of T_{wpt} to T_{frame} will be reduced because T_{pilot} cannot be changed to preserve the accuracy in the space domain. This may decrease the overall efficiency of the WPT. In this section, we propose a technique to improve the accuracy of the conventional beam-scanning scheme presented in Section II-B that does not involve altering the beam scanning resolution and frame duration.

A. SPATIAL INTERPOLATION

We used a TPS interpolation algorithm [24] to identify a more accurate AoD than that estimated using the conventional beam scanning algorithm. TPS interpolation utilizes the idea of an elastic shell and can adjust the smoothing level to establish a model for arbitrarily scattered data. A more accurate beam-steering AoD can be estimated by applying TPS interpolation to the beam scanning results.

The measured power z_{ij} corresponding to the AoD (θ_i, ϕ_j) estimated through beam scanning and a thin-plate physical model $f(\theta_i, \phi_j)$ are correlated as follows:

$$z_{ij} = f(\theta_i, \phi_j), \quad i = 1, 2, \ldots, K_e, \ j = 1, 2, \ldots, K_a. \quad (8)$$

Note that the function f is initially unknown and obtained as the outcome of the TPS interpolation. In other words, the purpose of the TPS interpolation is to find a function f that well describes the variation of the received power with θ and ϕ. In particular, the TPS model can be extracted by solving a mixed target minimization problem:

$$\min_{f} \sum_{i=1}^{K_e} \sum_{j=1}^{K_a} \left(z_{ij} - f(\theta_i, \phi_j)\right)^2 + \alpha E_b(f), \quad (9)$$

where the first term denotes the external energy that reflects the sum of squared errors between the fitted surface and the data, and $E_b(f)$ is the bending energy that acts as a roughness penalty. $0 \leq \alpha \leq 1$ is a parameter that controls the smoothing level, i.e., smoothness of the allowable deformation by changing the weight for the bending energy [25]. The higher α is, the less exact the fit to data becomes; If $\alpha = 0$, the data will be fit exactly, whereas, if α is close to 1, the solution tends to approximate the least-squares one. The bending energy $E_b(f)$ in (9) can be expressed as [26]

$$E_b(f) = \int_{-\infty}^{\infty} \int_{-\infty}^{\infty} \left[\left(\frac{\partial^2 f}{\partial \theta^2}\right)^2 + 2 \left(\frac{\partial^2 f}{\partial \theta \partial \phi}\right)^2 + \left(\frac{\partial^2 f}{\partial \phi^2}\right)^2 \right] d\theta d\phi. \quad (10)$$

The solution to the problem expressed in (9) can be obtained by solving a linear system of equations. Specifically, the TPS model f can be represented as

$$f(\theta, \phi) = \sum_{i=1}^{K_e} \sum_{j=1}^{K_a} \rho_{ij} o_{ij}^2 \ln o_{ij} + d_0 + d_1 \theta + d_2 \phi, \quad (11)$$

where θ and ϕ denote the elevation and azimuth angles, respectively, and $o_{ij} \triangleq \sqrt{(\theta - \theta_i)^2 + (\phi - \phi_j)^2}$, $i = 1, 2, \ldots, K_e$, $j = 1, 2, \ldots, K_a$. Subsequently, the function is determined using a set of $K + 3$ parameters: ρ_{ij} $(i = 1, 2, \ldots, K_e, j = 1, 2, \ldots, K_a)$, d_0, d_1, and d_2. These parameters can be computed by applying block Gaussian elimination to the following linear system of equations [27]:

$$\begin{bmatrix} \alpha & g_{12} & g_{13} & \cdots & g_{1K_a} & 1 & \theta_1 & \phi_1 \\ g_{21} & \alpha & g_{23} & \cdots & g_{2K_a} & 1 & \theta_2 & \phi_2 \\ \vdots & \vdots & \vdots & \vdots & \vdots & \vdots & \vdots & \vdots \\ g_{K_e 1} & g_{K_e 2} & g_{K_e 3} & \cdots & \alpha & 1 & \theta_{K_e} & \phi_{K_a} \\ 1 & 1 & 1 & \cdots & 1 & 0 & 0 & 0 \\ \theta_1 & \theta_2 & \theta_3 & \cdots & \theta_{K_e} & 0 & 0 & 0 \\ \phi_1 & \phi_2 & \phi_3 & \cdots & \phi_{K_a} & 0 & 0 & 0 \end{bmatrix} \begin{bmatrix} \rho_{11} \\ \rho_{22} \\ \vdots \\ \rho_{K_e K_a} \\ d_0 \\ d_1 \\ d_2 \end{bmatrix}$$
$$= \begin{bmatrix} z_{11} & z_{12} & \cdots & z_{K_e K_a} & 0 & 0 & 0 \end{bmatrix}^T, \quad (12)$$

where $g_{ij} \triangleq o_{ij}^2 \ln o_{ij}$ and $i = 1, 2, \ldots, K_e, j = 1, 2, \ldots, K_a$.

Using the estimated TPS model f, the elevation and azimuth angles of the beam steering can be expressed as

$$(\theta^*, \phi^*) = \underset{\theta \in [\hat{\theta} - \Delta\theta, \hat{\theta} + \Delta\theta), \phi \in [\hat{\phi} - \Delta\phi, \hat{\phi} + \Delta\phi)}{\mathrm{argmax}} f(\theta, \phi), \quad (13)$$

where $\hat{\theta}$ and $\hat{\phi}$ denote the steering AoD corresponding to the maximum average received signal strengths among the K candidate values obtained at the receiver. The problem in (13) is to find the optimal angles of θ and ϕ that maximize the energy transferred to the receiver, and it can be solved using an exhaustive search over a search space of two quantized AoDs centered at $\hat{\theta}$ and $\hat{\phi}$, as the optimal angles will be near the quantized angles $\hat{\theta}$ and $\hat{\phi}$. As a result, TPS interpolation identifies a more appropriate AoD (θ^*, ϕ^*) surrounding the initially estimated AoD obtained via beam scanning.

B. TEMPORAL INTERPOLATION

We propose an algorithm to estimate the moving path of the mobile receiver to update the steering AoD semi-continuously within the WPT section of the frame. The proposed scheme applies n-th-order polynomial interpolation across frames to the steering AoDs obtained via beam scanning with or without TPS. Note that the frame duration T_{frame} is fixed. Without temporal interpolation, the beamforming weight vector can be updated only once per frame. If we adopt the temporal interpolation as proposed in our paper, the moving path of the receiver is continuously estimated with a continuous function, and thus, the beamforming weight vector can be updated with infinite precision. However, too many updates will cause excessive complexity at the transmitter. We introduce U, which denotes the number

of updates of the beamforming weight vector within each frame interval, as a parameter to compromise between the update rate and complexity. As a result, using the n-th-order polynomial equation resulting from the interpolation, the beam-steering AoD of the transmitter is updated U times with a constant update period T_{update} within each frame along the estimated moving path. The parameter U determines the update frequency of the steering direction, and it is related to T_{wpt} and T_{update} as $U = T_{wpt}/T_{update}$.

Under the assumption that the receiver moves with time t on the xz-plane in Fig. 1, the n-th-order polynomials $p_x(t)$ and $p_z(t)$ for the location of the receiver in each axis can be written as

$$p_x(t) \triangleq q_{x0} + q_{x1}t + q_{x2}t^2 + \cdots + q_{xn}t^n,$$
$$p_z(t) \triangleq q_{z0} + q_{z1}t + q_{z2}t^2 + \cdots + q_{zn}t^n. \quad (14)$$

To estimate the n-th-order polynomial coefficients, beam scanning results for at least $n + 1$ consecutive frames are necessary. Using the data, the coefficients of the polynomials can be obtained through linear regression based on the least squares criterion. Specifically, let $\{t_1, t_2, \ldots, t_{n+1}\}$ and $\{(x_1, z_1), (x_2, z_2), \ldots, (x_{n+1}, z_{n+1})\}$ be the time sequence and the corresponding locations of the receiver measured at $n+1$ consecutive frames. Then, the sum of squared errors, S_x and S_z, are defined as

$$S_x \triangleq \sum_{i=1}^{n+1}(x_i - p_x(t_i))^2, \; S_z \triangleq \sum_{i=1}^{n+1}(z_i - p_z(t_i))^2. \quad (15)$$

Correspondingly, the least squares solutions for the coefficients $\{q_{x0}, q_{x1}, \ldots, q_{xn}\}$ and $\{q_{z0}, q_{z1}, \ldots, q_{zn}\}$ in (14) can be obtained as

$$\frac{\partial S_x}{\partial q_{xj}} = -2t_i^j \sum_{i=1}^{n+1}(x_i - p_x(t_i)) = 0, \quad j = 0, 1, \ldots, n,$$

$$\frac{\partial S_z}{\partial q_{zj}} = -2t_i^j \sum_{i=1}^{n+1}(z_i - p_z(t_i)) = 0, \quad j = 0, 1, \ldots, n, \quad (16)$$

which yields

$$
\begin{bmatrix} q_{x0} \\ q_{x1} \\ \vdots \\ q_{xn} \end{bmatrix} =
\begin{bmatrix}
n & \sum_{i=1}^{n+1} t_i & \cdots & \sum_{i=1}^{n+1} t_i^n \\
\sum_{i=1}^{n+1} t_i & \sum_{i=1}^{n+1} t_i^2 & \cdots & \sum_{i=1}^{n+1} t_i^{n+1} \\
\vdots & \vdots & \ddots & \vdots \\
\sum_{i=1}^{n+1} t_i^n & \sum_{i=1}^{n+1} t_i^{n+1} & \cdots & \sum_{i=1}^{n+1} t_i^{2n}
\end{bmatrix}^{-1}
\cdot
\begin{bmatrix} \sum_{i=1}^{n+1} x_i \\ \sum_{i=1}^{n+1} x_i t_i \\ \vdots \\ \sum_{i=1}^{n+1} x_i t_i^n \end{bmatrix},
$$

TABLE 1. Simulation parameters.

Parameters	Value
Signal frequency	5.8 GHz
PAA size ($M \times N$)	7×7
Distance between Tx and receiving plane	2 m
Tx antenna element gain	12 dBi
Rx antenna gain	11 dBi
Antenna spacing (d)	$\lambda/2$
Transmit power per element	38.7 dBm
Frame duration (T_{frame})	1000 ms
Each pilot signal duration (T_s)	1 ms
Number of weight updates per frame (U)	10

$$
\begin{bmatrix} q_{z0} \\ q_{z1} \\ \vdots \\ q_{zn} \end{bmatrix} =
\begin{bmatrix}
n & \sum_{i=1}^{n+1} t_i & \cdots & \sum_{i=1}^{n+1} t_i^n \\
\sum_{i=1}^{n+1} t_i & \sum_{i=1}^{n+1} t_i^2 & \cdots & \sum_{i=1}^{n+1} t_i^{n+1} \\
\vdots & \vdots & \ddots & \vdots \\
\sum_{i=1}^{n+1} t_i^n & \sum_{i=1}^{n+1} t_i^{n+1} & \cdots & \sum_{i=1}^{n+1} t_i^{2n}
\end{bmatrix}^{-1}
\cdot
\begin{bmatrix} \sum_{i=1}^{n+1} z_i \\ \sum_{i=1}^{n+1} z_i t_i \\ \vdots \\ \sum_{i=1}^{n+1} z_i t_i^n \end{bmatrix}. \quad (17)
$$

By estimating the coefficients $q_{x0}, q_{x1}, \ldots, q_{xn}$ of the polynomial $p_x(t)$ and $q_{z0}, q_{z1}, \ldots, q_{zn}$ of the polynomial $p_z(t)$, an expected moving path equation can be identified, and the position change of the receiver can be tracked continuously in the x-axis and z-axis, respectively. Accordingly, the beam-steering AoD that changes within the frame can be updated.

IV. NUMERICAL RESULTS
In this section, an evaluation of the performance of the proposed spatio–temporal interpolation technique is presented. A 7×7 PAA, i.e., $M = N = 7$, is considered, and the frequency of the transmit signal is set to 5.8 GHz. The frame duration and pilot signal duration for each steering AoD are set as $T_{frame} = 1000$ ms and $T_s = 1$ ms, respectively. The receiver is assumed to be located on a 5 m $\times$ 5 m receiving plane, located 2 m away from the transmitter. The ranges of the steering angles are assumed to be $\theta \in [-50°, 50°]$ and $\phi \in [-50°, 50°]$. The angular difference between adjacent beams is denoted as $\Delta\theta = 100°/2^{b_e}$, $\Delta\phi = 100°/2^{b_a}$, where b_e and b_a are the numbers of bits for the uniform quantization of the elevation and azimuth angles, respectively. Table 1 summarizes the parameters used in the simulations.

As performance measures, we consider the mean square error (MSE) of the beamforming weight estimation and WPT
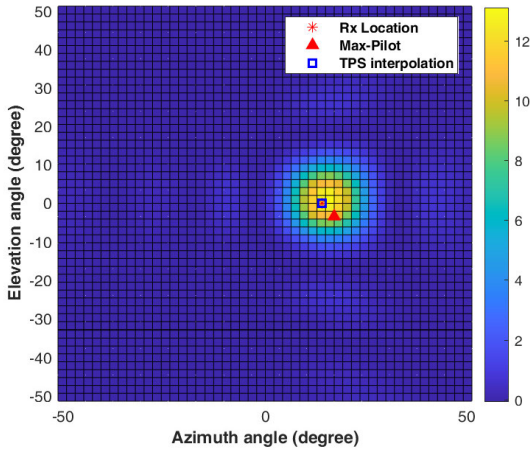
FIGURE 3. Steering angle estimation without and with TPS interpolation.

FIGURE 4. MSE of beamforming weights vs. the number of quantization bits.

FIGURE 5. WPT efficiency of beamforming weights vs. the number of quantization bits.

efficiency. The MSE is defined as

$$\text{MSE} = \frac{1}{2} E\left[\left(\beta(\theta_0, \phi_0) - \beta(\theta^*, \phi^*) \right)^2 \right], \quad (18)$$

where $\beta(\theta, \phi) \triangleq kd \cos\theta \sin\phi + kd \sin\theta \cos\phi$, and the WPT efficiency η is defined as the ratio of the received signal power to the transmit power:

$$\eta = \frac{P|\mathbf{h}^H \mathbf{w}(\theta_i, \phi_j)|^2 E[|s(t)|^2] + \sigma^2}{PE[|s(t)|^2]}. \quad (19)$$

A. EFFECT OF SPATIAL INTERPOLATION
We first validate the performance gain of TPS interpolation, assuming that the receiver is located at a fixed location. Fig. 3 shows the variation in the received power (in watts) as the steering elevation and azimuth angles of the pilot signal are swept over specified ranges. Each of the elevation and azimuth angles is quantized into 16 discrete angles, i.e., $b_e = b_a = 4$. The red asterisk in the figure indicates the actual receiver position, whereas the red square indicates the steering position corresponding to the maximum received power. This error is attributable to the quantization of the steering angles. The blue square indicates the steering position obtained via TPS interpolation. It is shown that the use of TPS interpolation improves the resolution of beam scanning, thereby providing a more accurate estimation of the receiver position than conventional beam scanning without interpolation ("Max-Pilot" in the figure).

Figs. 4 and 5 respectively show how the MSE in (18) and the WPT efficiency in (19) vary with the number of bits for the quantization of the steering angles. It is assumed that the total number of bits (b) is apportioned equally into the number of bits for the elevation angle (b_e) and azimuth angle (b_a), i.e., $b_e = b_a = b/2$. The elevation and azimuth angles of the receiver are assumed to be distributed uniformly over $[-50°, 50°)$. As the number of bits increases, the MSEs of both the conventional Max-Pilot and the proposed TPS interpolation schemes decrease owing to the increased resolution of beam scanning. The proposed TPS interpolation achieved
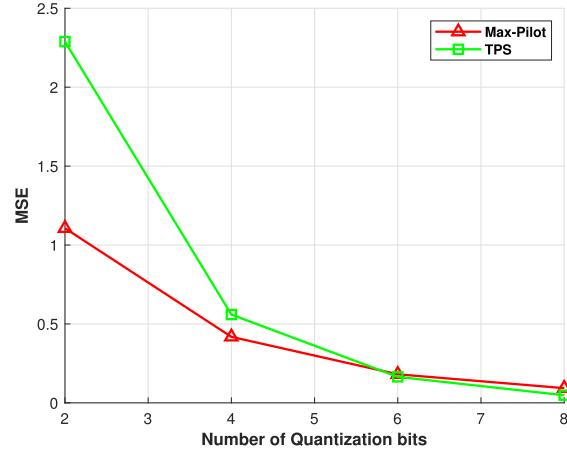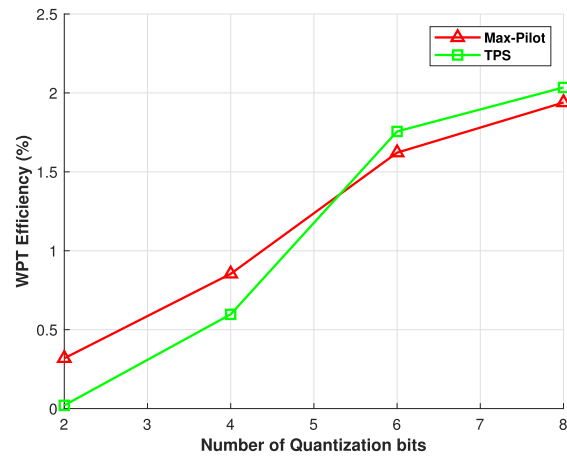
a lower MSE than the Max-Pilot scheme when $b \geq 6$. This implies that the number of bits for quantization should be sufficiently large to achieve an effective TPS interpolation; low-resolution beam scanning with only a few bits results in an inaccurate raw estimation, which cannot be overcome by TPS interpolation. A trend similar to that mentioned above was exhibited in the corresponding WPT efficiency, as shown in Fig. 5.

B. EFFECT OF TEMPORAL INTERPOLATION
In this section, we consider the receiver mobility. The receiver is assumed to move within a receiving plane on the xz-plane based on a coordinated turn model. The coordinated turn model models the motion of the target when it is assumed that the target rotates at a constant velocity in two-dimensional space. Let $\mathbf{g}(k) \triangleq [x(k), \dot{x}(k), z(k), \dot{z}(k)]^T$ be a vector representing the movement of the receiver at the k-th time instant, where $(x(k), z(k))$ denotes the location of the receiver and $(\dot{x}(k), \dot{z}(k))$ denotes the movement speed along each axis [28]. Then, $\mathbf{g}(k + 1)$ at the $(k + 1)$-th time instant is determined
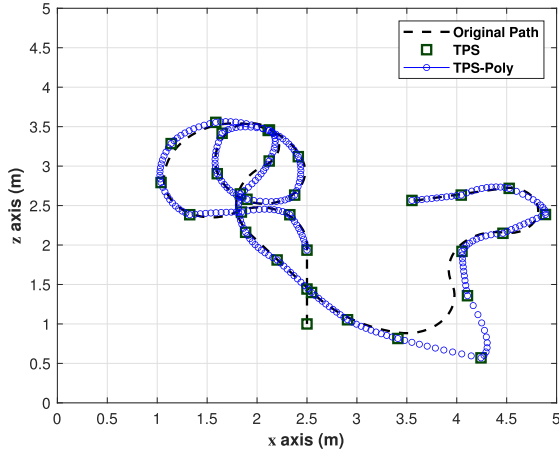
FIGURE 6. Original and estimated moving paths of receiver.

FIGURE 7. MSE of the beamforming weight estimation over time.

as [28]

$$
\mathbf{g}(k+1) =
\begin{bmatrix}
1 & \dfrac{\sin \Omega \Delta t}{\Omega} & 0 & -\dfrac{1 - \cos \Omega \Delta t}{\Omega} \\
0 & \cos \Omega \Delta t & 0 & -\sin \Omega \Delta t \\
0 & \dfrac{1 - \cos \Omega \Delta t}{\Omega} & 1 & \dfrac{\sin \Omega \Delta t}{\Omega} \\
0 & \sin \Omega \Delta t & 0 & \cos \Omega \Delta t
\end{bmatrix}
\mathbf{g}(k),
$$

(20)

where Ω denotes the angular velocity, and Δt is the interval between adjacent time instants. It is assumed that Ω follows a uniform distribution on $[-100, 100]$ °/sec and updated every two frames. The time interval Δt was set to 100 ms. We performed a comparison on the following three cases: no interpolation (Max-Pilot), spatial interpolation only (TPS), and spatio–temporal interpolation (TPS-Poly: TPS interpolation in space and polynomial interpolation in time) in terms of the MSE and WPT efficiency. For the temporal interpolation, we assumed a second-order polynomial model, i.e., $n = 2$.[1]

Fig. 6 shows the moving path estimated via the second-order polynomial interpolation, along with the original moving path. TPS interpolation was performed to estimate the receiver location in every frame, and the location of the receiver within each frame was updated $U = 10$ times based on the estimated moving path. The observations on the receiver location on the xz-plane corresponding to three preceding frames are used to estimate the polynomials for the moving path. For instance, the observations obtained by the TPS interpolation in the 2nd, 3rd, and 4th frames are (2.5000, 1.9354), (2.3282, 2.3840), and (1.8430, 2.4179), respectively, and the polynomials $p_x(t) = 3.590 - 0.3721t - 0.0161t^2$ and $p_z(t) = 1.876 + 0.271t - 0.0339t^2$ can be derived by solving (17). Using these polynomials, the location of the receiver and the corresponding beamforming

---

[1]The optimal order of the polynomial model depends on the movement model of the receiver. For the coordinated turn model in (20), we empirically discovered that $n = 2$ provides the best performance in most cases. Hence, we set $n = 2$ in our study.
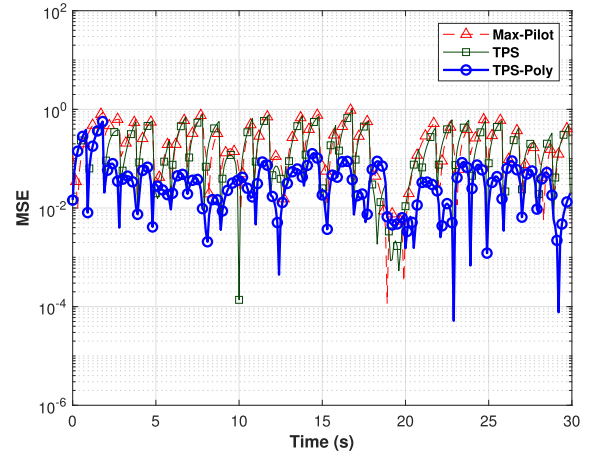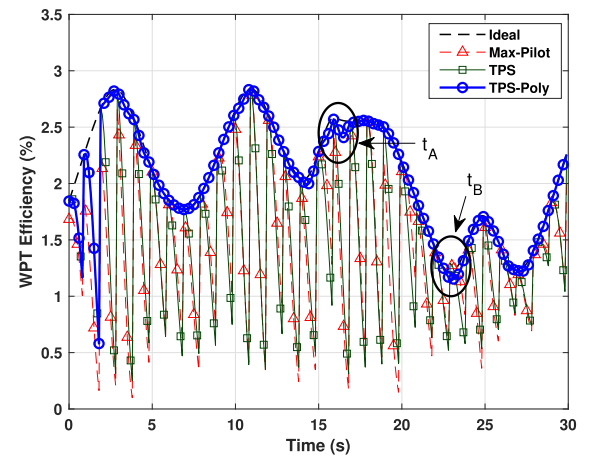

FIGURE 8. WPT efficiency over time.

weight vector are updated U times until the observation in the 5th frame is available. It is seen that the estimated moving path is typically consistent with the original path. In specific outer regions, however, the location estimated via TPS deviated significantly from the original moving path owing to the limited radiation pattern of the PAA; for certain steering angles far from the bore-sight, the angles associated with the maximum directional antenna gain tends to deviate from the intended steering angles. Consequently, the estimated moving path came to deviate from the original moving path.

Figs. 7 and 8 show how the MSE and WPT efficiency vary with time as the receiver moves following the original path shown in Fig. 6. The MSE and WPT efficiency are shown to fluctuate because the beamforming weight vector is updated in discrete times while the receiver location is continuously varying. Note that the MSE and WPT efficiency were not averaged out, that is, they are instantaneous values. The steering angles of beamforming were updated only once every frame in the cases of Max-Pilot and TPS, whereas they were updated $U = 10$ times in the

TABLE 2. Comparison of relative WTP efficiency.

Scheme	Max-Pilot	TPS	TPS-Poly	
Relative WPT Efficiency	71.83%	77.46%	U=2	91.58%
			U=5	94.74%
			U=10	96.36%

case of spatio–temporal interpolation. Owing to more frequent updates of the beam-steering angles due to the moving path estimation, the proposed spatio–temporal interpolation yielded a lower MSE and a higher WPT efficiency, particularly in time intervals across frames. It is worth mentioning that the higher update rate was implemented by temporal interpolation across frames, without changing the frame duration. The effect of the aforementioned relatively large errors in the moving path estimation during a short period on the WPT efficiency was marginal; the corresponding time sections are denoted as t_A and t_B in Fig. 8.

Table 2 summarizes the *relative* WPT efficiency of the three schemes, where the relative WPT efficiency of each scheme is defined as the WPT efficiency divided by that obtained with a perfect estimation of the moving path. This reflects the WPT efficiency in (19) and the accuracy of the path estimation at the same time. The efficiency was averaged over 1,000 independent realizations of random moving path that persists for 30 seconds. The superior performance of the proposed TPS-Poly scheme is attributed to higher update rate of the beamforming weight vector. As expected, relative WPT efficiency is shown to improve as the number of updates (U) increases. Remarkably, the proposed spatio–temporal interpolation achieves 96.43% of the ideal WPT efficiency for the case of $U = 10$.

V. CONCLUSION

We proposed a spatio–temporal interpolation technique to improve the beamforming accuracy in a WPT system based on beam scanning using beam-steered pilot signals. Spatial interpolation was performed to enhance the spatial resolution of beam scanning using a limited number of bits for quantization, whereas temporal interpolation was used to enhance the time resolution of beam scanning by continually tracking the moving path of the receiver. TPS interpolation and polynomial interpolation were adopted for spatial and temporal interpolations, respectively. Numerical simulations were performed to validate the performance gain of the proposed scheme in terms of the MSE of the beamforming weight vector and the WPT efficiency. It was discovered that the proposed spatio–temporal interpolation technique enhanced the beamforming accuracy without increasing the pilot overhead, resulting in significant improvements in the MSE and WPT efficiency. The fine beam steering method based on the proposed interpolation technique can be exploited in wireless communications as well as the WPT, e.g., unmanned aerial vehicle communications and inter-satellite optical communications.

REFERENCES

[1] G. A. Akpakwu, B. J. Silva, G. P. Hancke, and A. M. Abu-Mahfouz, "A survey on 5G networks for the Internet of Things: Communication technologies and challenges," *IEEE Access*, vol. 6, pp. 3619–3647, 2017.

[2] E. Hossain and M. Hasan, "5G cellular: Key enabling technologies and research challenges," *IEEE Instrum. Meas. Mag.*, vol. 18, no. 3, pp. 11–21, Jun. 2015.

[3] P. Popovski, K. F. Trillingsgaard, O. Simeone, and G. Durisi, "5G wireless network slicing for eMBB, URLLC, and mMTC: A communication-theoretic view," *IEEE Access*, vol. 6, pp. 55765–55779, 2018.

[4] W. Hong, Z. H. Jiang, C. Yu, J. Zhou, P. Chen, Z. Yu, H. Zhang, B. Yang, X. Pang, M. Jiang, Y. Cheng, M. K. T. Al-Nuaimi, Y. Zhang, J. Chen, and S. He, "Multibeam antenna technologies for 5G wireless communications," *IEEE Trans. Antennas Propag.*, vol. 65, no. 12, pp. 6231–6249, Dec. 2017.

[5] J. Ding, M. Nemati, C. Ranaweera, and J. Choi, "IoT connectivity technologies and applications: A survey," *IEEE Access*, vol. 8, pp. 67646–67673, 2020.

[6] L. Liu, E. G. Larsson, W. Yu, P. Popovski, C. Stefanovic, and E. de Carvalho, "Sparse signal processing for grant-free massive connectivity: A future paradigm for random access protocols in the Internet of Things," *IEEE Signal Process. Mag.*, vol. 35, no. 5, pp. 88–99, Sep. 2018.

[7] L. Xie, Y. Shi, Y. T. Hou, and W. Lou, "Wireless power transfer and applications to sensor networks," *IEEE Wireless Commun. Mag.*, vol. 20, no. 4, pp. 140–145, Aug. 2013.

[8] E. Waffenschmidt and T. Staring, "Limitation of inductive power transfer for consumer applications," in *Proc. 13th Eur. Conf. Power Electron. Appl. (EPE)*, Sep. 2009, pp. 1–10.

[9] I. Mayordomo, T. Dräger, P. Spies, J. Bernhard, and A. Pflaum, "An overview of technical challenges and advances of inductive wireless power transmission," *Proc. IEEE*, vol. 101, no. 6, pp. 1302–1311, Jun. 2013.

[10] F. Lu, H. Zhang, and C. Mi, "A review on the recent development of capacitive wireless power transfer technology," *Energies*, vol. 10, no. 11, p. 1752, Nov. 2017.

[11] J. Dai and D. C. Ludois, "A survey of wireless power transfer and a critical comparison of inductive and capacitive coupling for small gap applications," *IEEE Trans. Power Electron.*, vol. 30, no. 11, pp. 6017–6029, Nov. 2015.

[12] C. R. Valenta and G. D. Durgin, "Harvesting wireless power: Survey of energy-harvester conversion efficiency in far-field, wireless power transfer systems," *IEEE Microw. Mag.*, vol. 15, no. 4, pp. 108–120, Jun. 2014.

[13] A. Sample and J. R. Smith, "Experimental results with two wireless power transfer systems," in *Proc. IEEE Radio Wireless Symp.*, Jan. 2009, pp. 16–18.

[14] J. Huang, C.-C. Xing, and C. Wang, "Simultaneous wireless information and power transfer: Technologies, applications, and research challenges," *IEEE Commun. Mag.*, vol. 55, no. 11, pp. 26–32, Nov. 2017.

[15] R. Hansen, *Phased Array Antennas* (Wiley Series in Microwave and Optical Engineering). Hoboken, NJ, USA: Wiley, 2009.

[16] H. Li and B. Himed, "Transmit subaperturing for MIMO radars with co-located antennas," *IEEE J. Sel. Topics Signal Process.*, vol. 4, no. 1, pp. 55–65, Feb. 2010.

[17] K. Huang and X. Zhou, "Cutting the last wires for mobile communications by microwave power transfer," *IEEE Commun. Mag.*, vol. 53, no. 6, pp. 86–93, Jun. 2015.

[18] W. Chien, C.-C. Chiu, Y.-T. Cheng, W.-L. Fang, and E. H. Lim, "Multi-objective function for SWIPT system by SADDE," *Appl. Sci.*, vol. 10, no. 9, p. 3124, Apr. 2020.

[19] W. Zhang, Q. Yin, H. Chen, F. Gao, and N. Ansari, "Distributed angle estimation for localization in wireless sensor networks," *IEEE Trans. Wireless Commun.*, vol. 12, no. 2, pp. 527–537, Feb. 2013.

[20] H. Yomo and E. D. Carvalho, "A CSI estimation method for wireless relay network," *IEEE Commun. Lett.*, vol. 11, no. 6, pp. 480–482, Jun. 2007.

[21] R. Mudumbai, J. Hespanha, U. Madhow, and G. Barriac, "Distributed transmit beamforming using feedback control," *IEEE Trans. Inf. Theory*, vol. 56, no. 1, pp. 411–426, Jan. 2010.

[22] G.-M. Kang and O.-S. Shin, "A wireless power transfer system with beamforming based on beam-steered pilots," *J. Inst. Electron. Inf. Eng.*, vol. 57, no. 8, pp. 28–33, Aug. 2020.

[23] C. A. Balanis, *Antenna Theory: Analysis and Design*, 4th ed. Hoboken, NJ, USA: Wiley, 2016.

[24] W. Keller and A. Borkowski, "Thin plate spline interpolation," *J. Geodesy*, vol. 93, no. 9, pp. 1251–1269, Sep. 2019.

[25] F. Bai and A. Bartoli, "Procrustes analysis with deformations: A closed-form solution by eigenvalue decomposition," *Int. J. Comput. Vis.*, vol. 130, no. 2, pp. 567–593, Feb. 2022.

[26] V. Balek and I. Mizera, "Mechanical models in nonparametric regression," *Inst. Math. Statist. Collections*, vol. 9, pp. 5–19, Jan. 2013.

[27] N. J. Higham, "Gaussian elimination," *WIREs Comput. Statist.*, vol. 3, no. 3, pp. 230–238, May/Jun. 2011.

[28] X. Yuan, F. Lian, and C. Han, "Models and algorithms for tracking target with coordinated turn motion," *Math. Problems Eng.*, vol. 2014, pp. 1–10, Jan. 2014.

GIL-MO KANG received the B.S., M.S., and Ph.D. degrees in electronic engineering from Soongsil University, Seoul, South Korea, in 2013, 2015, and 2021, respectively.

Since 2013, he has been with the Wireless Communications Laboratory, Soongsil University. He received the Global Ph.D. Fellows Scholarship from the National Research Foundation of Korea, in 2016, 2017, 2018, and 2019. His research interests include wireless communications, with particular focus on device-to-device communications, beamforming, 5G systems, and V2X communications.

HYEON MIN KIM (Member, IEEE) received the B.S. and Ph.D. degrees in electronic engineering from Soongsil University, Seoul, South Korea, in 2012 and 2022, respectively.

Since 2012, he has been with the Wireless Communications Laboratory, Soongsil University. His research interests include wireless communications, with particular focus on device-to-device communications, 5G systems, and signal processing.

OH-SOON SHIN (Member, IEEE) received the B.S., M.S., and Ph.D. degrees in electrical engineering and computer science from Seoul National University, Seoul, South Korea, in 1998, 2000, and 2004, respectively.

From 2004 to 2005, he was a Postdoctoral Fellow with the Division of Engineering and Applied Sciences, Harvard University, MA, USA. From 2006 to 2007, he was a Senior Engineer with Samsung Electronics, Suwon, South Korea. In 2007, he joined the School of Electronic Engineering, Soongsil University, Seoul, where he is currently a Professor. His research interests include communication theory, wireless communication systems, and signal processing for communications.

KI-WON PARK (Student Member, IEEE) received the B.S. degree in electronic engineering from Soongsil University, Seoul, South Korea, in 2020, where he is currently pursuing the M.S. degree with the Department of Information and Telecommunication Engineering.

Since 2020, he has been with the Wireless Communications Laboratory, Soongsil University. His research interests include wireless communications, with particular focus on wireless power transfer, beamforming, and 5G communications.

● ● ●